Effectiveness of Cross-Walls in Reducing Wall Deflections in Deep Excavations

L. W. Wong[1*], R. N. Hwang[2]

[1]Formerly Moh and Associates, Inc., Taipei

[2]Moh and Associates, Inc., Taipei

*Corresponding author

doi: https://doi.org/10.21467/proceedings.126.29

Abstract

Three cross-walls were installed to brace the diaphragm walls prior to excavation for a cross-over tunnel of the Taipei Metro in front of the South Gate of the old Taipei City and has now been a National Heritage. The tunnel had the maximum excavation depth of 20.1 m. Three-dimensional finite element analyses have been performed to evaluate the effectiveness and the influence of the cross-walls in reducing the wall deflections. The nonlinear Hardening-Soil model has been adopted in the analyses. The results of the analyses indicate that the maximum wall deflections are much reduced as a result and the effectiveness of cross-walls is thus proved.

Keywords: Deep excavation, Cross wall, 3D analysis, Taipei MRT

1 Introduction

Cross-walls is common construction method for protecting structures adjacent to deep excavations. Eide et al. (1972) developed the concept for improving bottom heave stability and limiting displacements in deep excavations using diaphragm walls to act as cross-walls below the final excavation level. Karlsrud and Andresen (2008) reported 4 case histories on using cross-walls to reduce displacements for excavation in soft normally consolidation Oslo clay. Ou et al. (2006) reported the use of cross-walls to reduce the displacements for a 32.5 m deep excavation in soft clay in Taipei. Although these case histories show that cross-walls are very effective in reducing lateral displacements of diaphragm wall, the design methodology has not been fully developed.

Presented herein is a study of the effectiveness of cross-walls in reducing the deflections of the diaphragm walls to reduce the potential damages to a historical monument, i.e., Lizhenmen, refer to Figure 1, which is the South Gate (the Gate, hereinafter) of the old Taipei City built in Ching Dynasty in 1884. The Gate was designated as a Class I heritage of the City in 1998. Since it is close to the excavation for constructing a cross-over tunnel of the Taipei Metro, three cross-walls were installed prior to the commencement of excavation to reduce the movements of the diaphragm walls.

Proceedings DOI: 10.21467/proceedings.126; Series: AIJR Proceedings; ISSN: 2582-3922; ISBN: 978-81-954993-7-3

Figure 1: Lizhengmen, South Gate of Old Taipei City

While the 3 cross-walls are deployed symmetrically against the central axis of the Gate, two-dimensional (2D) finite element analysis could be conducted along the axis of the Gate to study the effectiveness of the cross-walls. The equivalent stiffness values for the soil and the cross-wall materials could be adopted to study the effects to wall deflections and to compare the performance with and without cross-walls. However, since the 2D model assumes that the cross-walls extend infinitely along the longitudinal direction, it could not analysis the variation in wall deflections with the distances to the cross-walls, nor to assess the wall deflections between 2 cross-walls. In order to study the influence of the cross-walls, the three-dimensional (3D) finite element analyses have been conducted in this study. As soils are nonlinear materials, the Hardening-Soil (HS) constitutive model is adopted to simulate the non-linear stress-strain relationships of soils. The various parameters for the HS model are calibrated against the deflection profiles observed in Inclinometer SID-6, which is located far away from the end walls or from the cross-walls so that the 2D analysis could be adopted. The set of calibrated parameters is then applied for the 3D analysis for the cross-walls. The 3D analyzed deflection profiles are compared with those observed in 2 inclinometers, namely, SID-2 and SID-3 for validation. Since these inclinometers were installed to the same depths as the diaphragm walls, their readings were duly corrected to account for the movements at the wall toes.

2 Case Studied

2.1 Cross-Over Tunnel

The cross-over tunnel, refer to Figure 2, running between Xiaonanmen Station and Chiang Kai Shek (CKS) Memorial Hall Station of the Taipei Metro, was constructed by using the cut-and-cover method. The length of the tunnel is 397 m and the widths of the tunnel vary from 13 m to 8 m. The depths of excavations increase from 16.5 m at the west end to 21.7 m at the east end. This section of the route could be considered as free-field for evaluating the influences of various parameters on wall deflections because there are only a few low-rise structures in the vicinity of the excavation with one-level basements under some of them. Therefore, wall deflections are in general unaffected by the presence of adjacent structures. As such, the readings obtained by Inclinometer SID-6, which is 210 m from the Gate, can be used to compare with the results obtained in the free-field analyses for calibrating the soil parameters adopted.

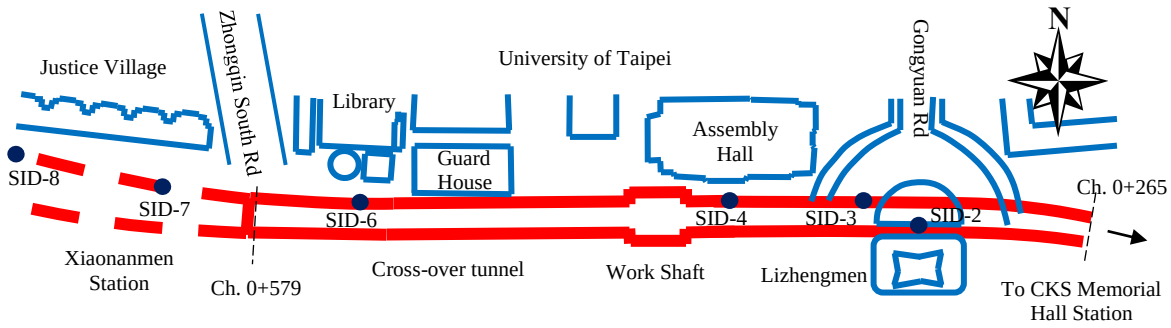

Figure 2: The cross-over between Xiaonanmen Station and Chiang Kai Shek Memorial Hall Station

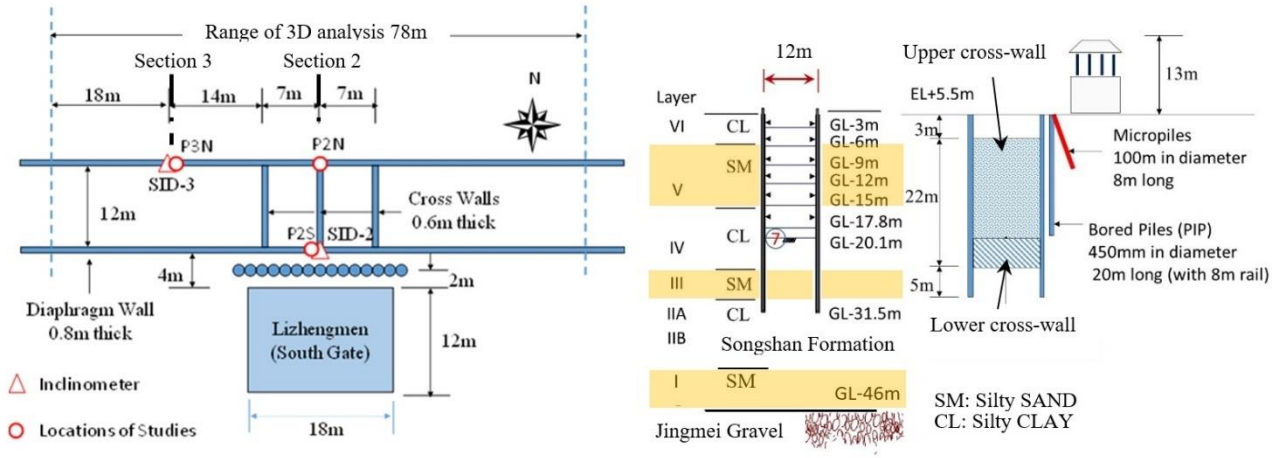

Figure 3: Layout and cross-section of the cross-walls for protecting Lizhenmen and locations of interest

Near the Gate, the excavation was carried out to a maximum depth of 20.1 m in 7 stages. The pit was retained by diaphragm walls of 0.8 m in thickness with the depths varying from 30 m to 32 m. The walls were braced by 6 levels of steel struts spaced at 3 m intervals. The un-reinforced cross-walls were built by the diaphragm walling technique along the transverse direction of the tunnel. Since the influences of the Gate and the cross-walls on the wall deflections are the main theme of the current study, the 3D analyses performed are limited to a section of the route of 78 m in length as depicted in Figure 3. It is considered that the influence of the excavation is approximately 1.5 times the excavation depth in the T2 Zone. The lateral extent of the numerical model along the east-west direction is taken as 30 m from each side of the Gate of 18 m in width. Along the north-south direction, the lateral extent is taken as 34 m each side from the excavation trench of 12 m in width. The model therefore has the dimension of 78 m by 80 m. Figure 9 depicted the western half of the 3D finite element model.

The readings obtained by Inclinometer SID-2 in front of the Gate are of primary interest and are compared with the results of the 3D analyses at the corresponding location, i.e., P2S. The results of the analyses obtained at Location P3N are also compared with the readings obtained by Inclinometer SID-3 to assess the influence of the cross-walls.

Proceedings DOI: 10.21467/proceedings.126
ISBN: 978-81-954993-7-3

Series: AIJR Proceedings
ISSN: 2582-3922

2.2 Ground Conditions

This section of the tunnel route is located in the T2 Zone (MAA 1987; Lee 1996) in the central Taipei Basin. As depicted in the cross-section in Figure 3, the Songshan Formation at the surface comprises six alternating sand (SM) and clay (CL) layers i.e., sublayers I, III and V of sandy soils and sublayers II, IV and VI of clayey soils. Underlying the Songshan Formation is a water-rich gravelly (GM) stratum, i.e., the so-called Jingmei Formation. The properties of the six sublayers in the Songshan Formation have been well discussed in literatures (Moh and Ou 1979; MAA 1987).

The piezometric levels in the Jingmei Formation were lowered to a level near the bottom of the Songshan Formation in the 1970s due to excessive extraction of groundwater as the sole water supply for the city, leading to significant reductions of water pressures in the Songshan Formation and substantial ground settlements as a result. The piezometric levels in the Jingmei Formation did not recover till the mid-1970s although pumping had been banned since 1968. The subsoils in the Songshan Formation in the central city area are thus substantially over-consolidated. This is particularly true for the clayey sublayer II because the underlying sandy sublayer I is so permeable that the piezometric level in sublayer I essentially dropped by the same magnitudes as those in the Jingmei Formation.

An advanced study was conducted by Geotechnical Engineering Specialty Consultant engaged by the Department of Rapid Transit Systems of Taipei City Government in the very early stage of the metro construction. The Designated Task studied the characteristics of the soils in the Taipei basin to provide the basic information for the design and construction of metro facilities (Chin et al. 1994; Chin and Liu 1997). Soilsamples of high quality were obtained and tested under stringent supervision. Hwang et al. (2013) summarized the results of the study and suggested Figure 4 be adopted for estimating undrained shear strengths of the clays in the central city areas, including the T2 Zone, for practical applications.

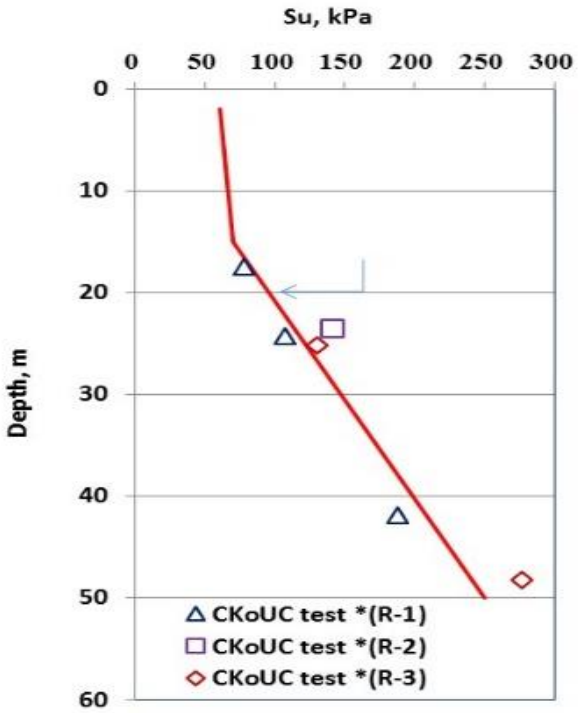

Figure 4: Estimated undrained shear strengths of clays in T2, TK2 and K1 Zones (Hwang et al. 2013)

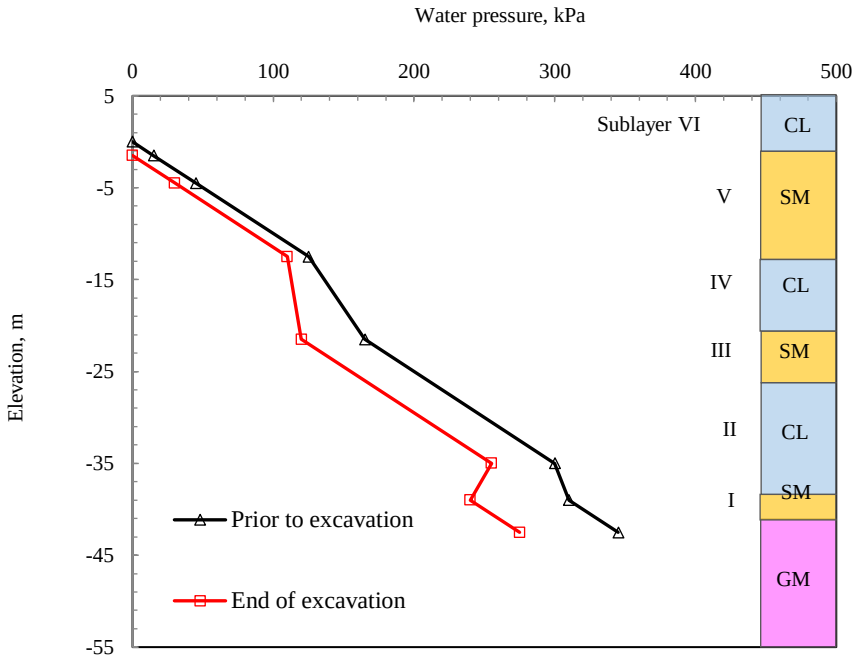

Figure 5: Groundwater pressures on the outer face of the diaphragm walls

2.3 Soil Parameters for Hardening-Soil model

The PLAXIS-3D finite element software developed by PLAXIS BV (2013) has become a very popular tool in geotechnical analysis and design. The Hardening-Soil (HS) constitutive soil model (Schanz and Vermeer 1978; Schanz et al. 1989) introduced in the PLAXIS programme is adopted to simulate the non-linear behavior of soils under loading. In the HS model, different stiffness values are used to define the hyperbolic stress-strain relationship. The parameters for the HS soil model are:

E^{ref}_{50} is the reference secant stiffness from standard triaxial test,
E^{ref}_{oed} is the reference tangent stiffness for oedometer primary loading,
E^{ref}_{ur} is the reference unloading-reloading stiffness,
m is the exponential factor for stress-level dependency of stiffness,
R_f is the failure ratio, $R_f = q_a / q_f$,
q_f is the asymptotic value of the shear strength and q_a is the failure strength.

The stress-strain curves could be determined from laboratory tests such as the Ko-consolidated triaxial undrained compression and extension tests. In this study, the stiffness values of soils are related to the undrained shear strengths for clays and to the N values for sands. The empirical relationships expressed in Equations 1 to 4 are adopted in the analysis using the HS soil model:

$$E^{ref}_{50} = 250\, s_u \text{ (for clayey soils)} \quad (1)$$

$$E^{ref}_{50} = 2\, N \text{ (in MPa for sandy soils)} \quad (2)$$

$$E^{ref}_{ur} = 6\, E^{ref}_{50} \quad (3)$$

$$E^{ref}_{oed} = E^{ref}_{50} \quad (4)$$

in which s_u is the undrained shear strengths for clayey soils and N is the blow-counts in standard penetration tests for sandy soils. The soil parameters adopted in the finite element analyses are summarized in Table 1.

Proceedings DOI: 10.21467/proceedings.126
ISBN: 978-81-954993-7-3

Series: AIJR Proceedings
ISSN: 2582-3922

Equations 1 to 4 are basically obtained by back-analysis and by matching the deflection profiles observed in the inclinometers SID-2, SID-3 and SID-6. The effective shear strength parameters, i.e., the c′ and □′ values, for the silty sand strata, are determined from laboratory tests conducted on thin-wall tube specimens. For the clayey layers, $c' = s_u$ and □′ = 0° are assumed in the analyses. The dilation angle, □′, of 2°, 0° and 5° are adopted for the sandy, the clayey and the gravelly soils respectively. The interface reduction factor, R-inter, of 1.0 is adopted.

Table 1. Soil parameters for the HS model adopted in the PLAXIS analyses

Depth m	Soil type	Unit weight γ′ kN/m³	N value	Undrained shear strength s_u, kPa	Effective cohesion c′ kPa	Effective friction angle □′ deg	Dilation angle □′ deg	Reference stiffness, MPa		Poisson's ratio υ′
								Secant stiffness E^{ref}_{50}	Unload-reload stiffness E^{ref}_{ur}	
0-6	CL	18.8	4	50			0	12.5	37.5	0.35
6-17	SM	19.2	5		0	32	2	10	30	0.30
	SM	19.2	8				2	16	48	0.30
	SM	19.2	11				2	22	66	0.30
17-21	CL	18.6	6	53.7			0	13.4	40.2	0.35
21-25	CL	18.6	17	114.3			0	28.6	85.8	0.35
25-31	SM	19.4	18		0	32	2	36	108	0.30
31-39	CL	18.9		195.0			0	48.6	145.8	0.35
39-44	CL	18.9		241.0			0	60.2	180.6	0.35
44-46	SM	19.7	30		0	32	2	60	180	0.30
46-60	GM	19.9	>100		0	40	5	250	750	0.35

2.4 Groundwater Pressures

Piezometers were available in the Jingmei Formation and in the sandy sublayers in the Songshan Formation for monitoring the groundwater pressures. It was observed that prior to excavation, the piezometric levels in the Jingmei Formation, sublayer III and sublayer V were at EL. -9.0 m, EL. -5.0 m and EL. 0 m respectively. As depicted in Figure 5, the piezometric levels outside the diaphragm wall box in the Jingmei Formation, sublayer III and sublayer V dropped to EL. -15.0 m, EL. -9.5 m and EL. -1.5 m respectively at the end of excavation. Inside the pit, the groundwater levels lowered to 1 m below the excavation levels have been adopted in analyses.

3 Two-Dimensional Analyses on Free-Field Excavations

3.1 Effect of Over-Excavation and Delay in Strutting

To start with, 2D analyses are performed for calibrating the soil parameters adopted by comparing the wall deflections computed with those observed in Inclinometer SID-6. This inclinometer is located at 210 m west of the Gate and at 40 m east of the end wall of Xiaonanmen Station as depicted in Fig. 2. As these distances are more than 3 times the width of excavation of 12 m, the observed wall deflections would not likely be affected by the end walls or the cross-walls. The excavation to a depth of 17.8 m at the location of SID-6 was supported by 5 levels of struts S1 to S5, of which the properties are presented in Table 2.

Excavations mainly comprise 2 activities, namely, digging of soils and installation (including preloading) of struts. They are usually carried out by two different subcontractors and are carried out

zone by zone. Once the desired depth is reached in each stage, the subcontractor for digging will move to the next zone to keep on digging. The subcontractor for struts installation will then move in to install the struts. This sequential construction essentially creates a three-dimensional (3D) effect on the performance of the bracing system.

Although the construction sequences are normally specified in the designs, in reality, the sequence of excavation is at the contractors' discretion with considerations given to the progress of the works and resource allocations. Due to the lack of the knowledge on how the excavation is to be carried out, this 3D effect is usually ignored by the designers and the excavation in each stage is assumed to be carried out in one shot; and all the struts at the same levels are assumed to be installed and preloaded at the same time. As a result, the wall deflections tend to be over-estimated. The same holds true in back-analyses. However, if the design is conducted by using the parameters calibrated by back-analyses of previous case histories, the errors made in the back-analyses and the forward analyses would be mutually compensating to each other and the results computed would be suitable for design.

While it is common to specify that excavation shall be carried out to a depth of 1 m below the strut level, over-excavation by 1 m could also be specified to obtain sufficient space below the struts for moving excavators. The effect of over-excavation to wall deflections is taken into account in parameters calibration in this study.

Table 2. Strut properties

Strut level	Depth m	Strut type	Area A_s , cm^2	Stiffness E_sA_s/s, MN/m	Design preload, kN/m	Strut spacing s, m
S1	2.2	1H350x350x12x19	173.9	1,188	120	3.0
S2	5.2	1H400x400x13x21	218.7	1,494	250	
S3	8.2	2H350x350x12x19	347.8	2,377	500	
S4	11.0	2H350x350x12x19	347.8	2,377	500	
S5	14.2	2H400x400x13x21	437.5	2,989	553	
S6	17.0	2H400x400x13x21	437.5	2,989	500	

3.2 Effect Of Relaxation of Preloads in Struts

Another important factor, which is very influential to the results of analyses but is often overlooked, is the relaxation of the preloads in struts. In numerical analyses, the struts at the same level are usually assumed to be preloaded at the same time. However, in reality, the struts are preloaded one by one. As one strut is preloaded, the neighboring struts which had already been preloaded are somewhat relaxed and the loads in the struts would be dropped by a certain extent. Besides, the preloads in struts may be relaxed due to many other reasons, such as creeping of soils and/or changes in temperature. Therefore, the preloads shall be reduced in analyses to account for the loss to obtain more realistic results (Hwang and Wong 2018a; Hwang et al. 2018b).

To investigate the effects of over-excavation and loss of preloads to wall deflections, 5 cases are analyzed as summarized in Table 3. In Cases 1a to 1c, the excavation is assumed to stop at a depth of 1 m below the strut levels as normally specified in the design and in Cases 2a and 2b, an over-excavation of 1 m is assumed. The preloads applied on struts in different cases are as depicted in the table.

Proceedings DOI: 10.21467/proceedings.126
ISBN: 978-81-954993-7-3

Series: AIJR Proceedings
ISSN: 2582-3922

With 1 m over-excavation, i.e., excavating to a depth of 2 m below the strut levels, the wall deflections computed for the cases with the struts loaded to 100 % (Case 2a) and 50 % (Case 2b) of the design preloads are presented in Figures 6b and 6c. The wall deflections computed for the 3 cases without over-excavation are depicted in Figure 7 for comparison. The computed maximum wall deflections and the movements at the toes of the diaphragm walls for the two series of cases are compared in Table 3. It is obvious that over-excavation increases the maximum wall deflections by 4 mm to 5 mm and a relaxation of preloads in struts of 50 % would have a similar effect. Completely omission of the design preload would cause further 5 mm wall deflections. This trend of increasing in wall deflections due to the loss of preloads is in agreement with the findings presented in Hwang and Wong (2018a).

Table 3. Comparison of wall deflections with different strut preloads

Case number		Depth of excavation below strut levels, m	Strut preloading, %	Wall deflection in final stage, mm		
				Maximum	Increment due to loss in strut load	Toe
1	1a	1.0	100	33.0	-	5.4
	1b		50	37.7	4.7	5.4
	1c		0	43.0	10.0	5.3
2	2a	2.0	100	36.9	-	4.7
	2b		50	41.0	4.1	4.7

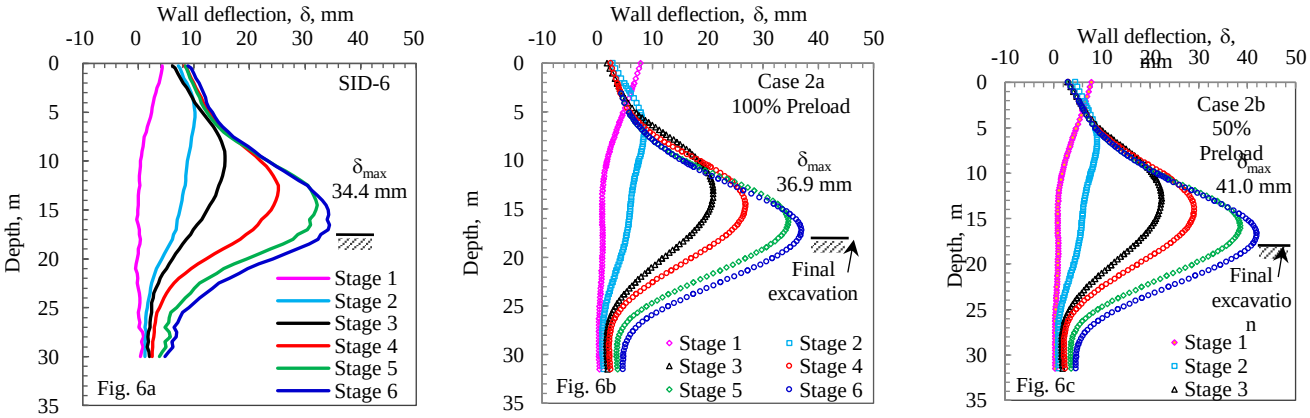

Figure 6: Observed and computed wall deflections with different preloads with over-excavation by 1 m

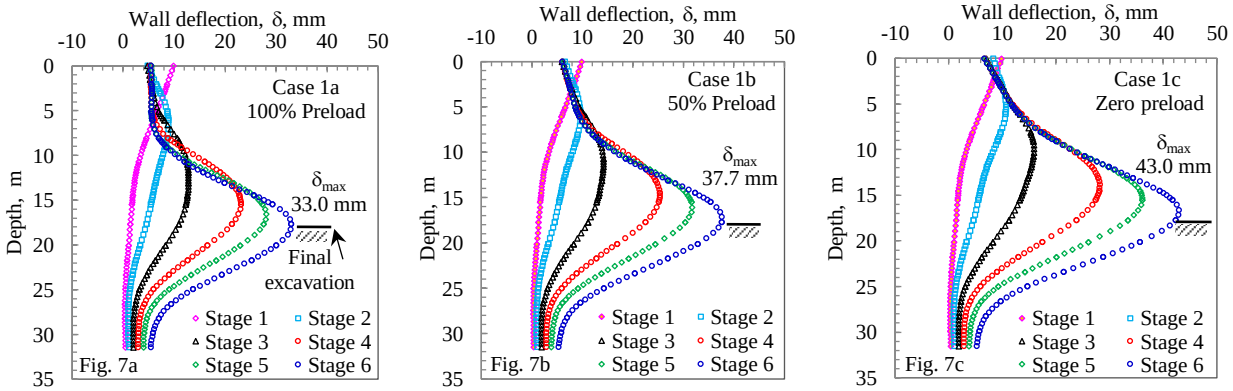

Figure 7: Computed wall deflections for struts with different preloads with normal excavation

3.2.1 Toe Movements of the Walls and Correction of Inclinometer Readings

The tips of the inclinometers shall be embedded in competent stratum, for instance, the Jingmei Gravel, so that the tips can be taken as the reference points for interpreting the readings. The tips of

inclinometers installed along the cross-over tunnel were however stopped at the toes of the diaphragm walls. The alternative of surveying the movements at the tops of the inclinometers and adopting the tops as the reference points was not conducted neither. In order to correctly interpret the inclinometer profiles, Hwang et al. (2007) proposed to correct the inclinometer readings by assuming the ends of the first-level struts to be unmoved once these struts are preloaded.

Figure 8 compares the deflection profiles at the end of the excavation for 0 %, 50 % and 100 % preloads, with and/or without over-excavation. The wall deflections above the final depth of excavation of 17.8 m are drastically affected by the magnitudes of the preloads. At the first struts level of 3 m depth, Figure 8 show that the wall deflections range from 4 mm to 10 mm for the various preloading cases in the final stage. However, as summarized in Table 3, the toe movements in the final stage are rather unaffected and range from 4.7 mm to 5.4 mm, with the differences less than 1 mm among the various preloading cases. This finding is useful as the diaphragm wall toes can be taken as the reference points for adjusting the inclinometer readings instead of using the ends of the first-level struts. Accordingly, the inclinometer readings for SID-6, SID-2 and SID-3 are adjusted based on the toe movements obtained from the numerical analysis.

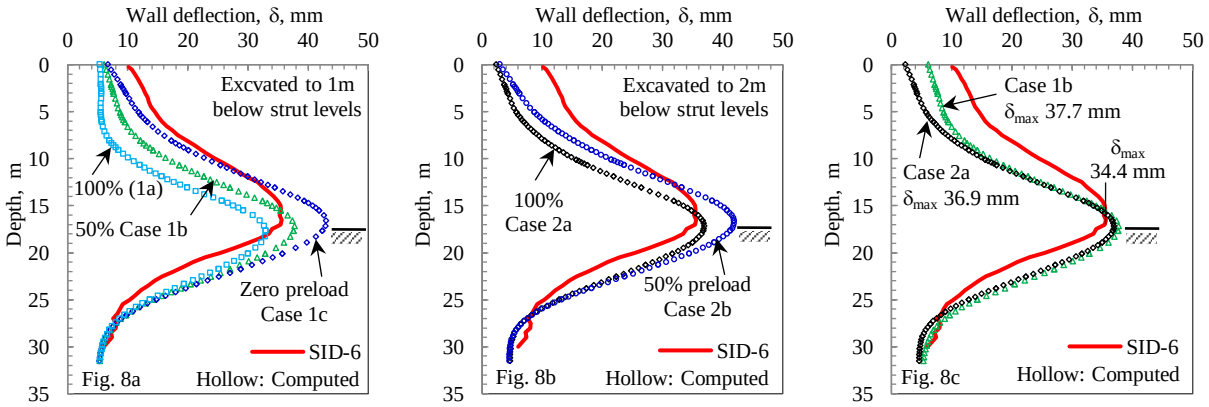

Figure 8: Computed wall deflections in the final stage of excavation with different preloads

3.3 Calibration of the Results Against the Readings Obtained by Inclinometer SID-6

As shown in Figure 8c, the computed deflection profiles for Cases 1b and Case 2a fit better with that observed by SID-6 shown in Figure 6a. The performance of the case excavated to 1 m below the strut levels with 50 % strut preloads would be quite similar to that excavated to 2 m below the strut levels with 100 % preloads. The effect to wall deflections caused by over-excavation is compensated by applying 100 % strut preloads. As a general rule, it is thus recommended in designs and in back-analysis to adopt 50 % of the design preloads with no over-excavation unless there are data to prove otherwise.

The agreement between the computed deflections with the readings obtained from SID-6, duly corrected to account for toe movements, validates the use of the soil parameters shown in Table 1 in numerical analyses.

4 Three-Dimensional Analysis on Cross-Walls

4.1 Modeling of the Gate

Figure 9 shows the 3D finite element model adopted in the analyses on the cross-walls. Although only the western half of the model along the longitudinal direction is shown, a full model is adopted in the

Proceedings DOI: 10.21467/proceedings.126
ISBN: 978-81-954993-7-3

Series: AIJR Proceedings
ISSN: 2582-3922

analyses. The full model is 60 m in depth, 80 m in the transverse direction and 78 m in the longitudinal direction of the cross-over tunnel. As shown in Figure 1, the lower portion of the Gate is a castle built by using large blocks of rock of 400 mm x 400 mm x 800 mm. The foundation of the Gate is also made of blocks of rock of similar size.

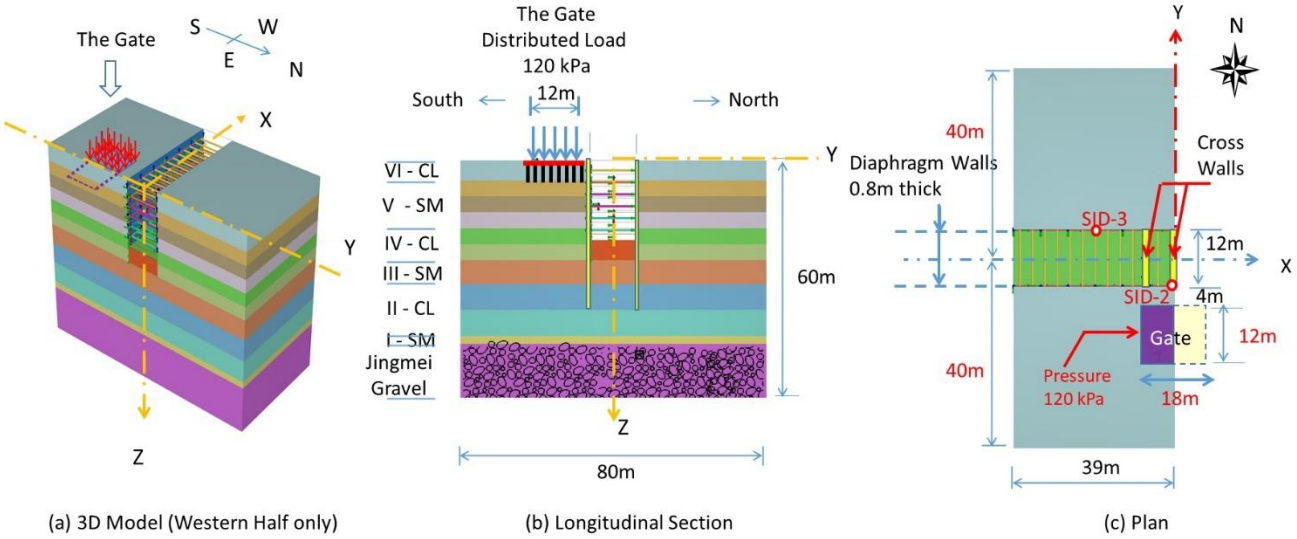

Figure 9: Western half of the 3D finite element model for numerical analyses using PLAXIS

The upper portion of the Gate was originally a masonry structure of a typical old Chinese style and was replaced by a pavilion in 1966. The castle is about 6 m in height and 12 m by 18 m in plan. It is conceivable that the foundation extends 2 m beyond the footprint of the castle, giving an area of 16 m by 22 m in plan dimensions. With due consideration given to the hallway and the empty spaces inside the castle, the surcharge load from the castle, including the weights of castle, the pavilion and the foundation, is estimated to be around 120 kPa. In consideration of the integrity of the castle and the rubbles foundation, the surcharge load 120 kPa is assumed to apply on a plate element of 0.8 m in thickness with an E value of 36 MPa. Analyses have shown that the rigidity of the plate has no influences on the wall deflections.

Because of the insufficient bearing capacity of the upper soil layers, timber piles were used to support the Gate. Li (2011) reported that timber piles of 3 m to 5 m in length were part of the foundation for a section of the masonry wall exposed at a nearby metro tunnel. For simplicity, these piles are considered as ground treatment in the finite element analyses. Timber piles of 200 mm in diameter are assumed to be installed at 0.6 m spacings to a depth of 6 m. The area ratio of the piles to soil mass is thus about 8.7 %. The E values of hardwoods range from 8 GPa to 15 GPa, and a value of 10 GPa is assumed to be representative. Accordingly, the equivalent E value of the treated soil mass would roughly be 1 GPA. The Poisson's ratio for the treatment zone is assumed to be 0.25.

4.2 Modeling of the Supporting Structures

The diaphragm walls are simulated by plate elements and an E_c value of 25,000 MPa is adopted for concrete with a characteristic compressive strength, i.e., f'_c value, of 28 MPa. The estimated flexural rigidity (denoted as E_cI_c where I_c is the moment of inertia) and the axial stiffness (denoted as E_cA_c where A_c is the sectional area) of the diaphragm wall are 750 MN-m and 14,056 MN/m respectively.

These values are reduced by 30 % for accounting tensile cracks and creeping of concrete during excavation.

Struts are represented by node-to-node anchors. The steel is assumed to be an elastic material with Young's modulus of the steel strut (E_s) of 210 GPa. The structural properties of the struts are shown in Table 2. As mentioned in Section 3.4, the inputted preloads in the struts are reduced by half of those specified in Table 2 in the 3D analyses. The horizontal spacing of the struts (s) is 3.0 m.

4.3 Modeling of the Cross-Walls

The un-reinforced cross-walls were constructed by the diaphragm walling method. They were cast into the upper and the lower portions as depicted in Figure 3. The upper portions of these cross-walls, poured at the depths between 3 m and 20.1 m, were supposed to be demolished as the excavation proceeded. Therefore, concrete with a very low strength was used. The lower portions, located at the depths between 20.1 m and 25 m, were cast by using normal low-grade concrete.

The 3 cross-walls are modeled as plate elements with the thicknesses of 600 mm. Data are unavailable for estimating the properties of the lean concrete used to cast these cross-walls. In the lack of information, the E value for both the upper and the lower portions of 700 MPa is adopted in analyses. This E value would be validated by comparing the results of the analyses with the readings of Inclinometer SID-2.

5 Results of 3-Dimensional Analyses

5.1 Scenarios Analyzed

The wall deflections obtained at the two ends of the cross-walls in front of the gate, i.e., Locations P2S and P2N (refer to Figure 3 for locations), are of primary interest for evaluating the effectiveness of the piles and the cross-walls in reducing wall deflections. As summarized in Table 4, four scenarios are analyzed to study the effects of the surcharge of the Gate to wall deflections with and without the cross-walls. The computed deflection profiles are presented in Figure 10 to Figure 12.

Firstly, analyses are performed for Scenario 1 in which the excavation is assumed to be conducted in the free-field, i.e., without the Gate nor the cross-walls. The computed wall deflection profiles at Location P2S are given in Figure 10a. A maximum deflection of 34.2 mm is computed as the excavation reached the final depth of 20.1 m. The toe movement at the depth of 31 m is 5.1 mm. Because of symmetry in geometry, the performance of the north wall is the same as that of the south.

The surcharge load of 120 kPa from the Gate increases the maximum deflection of the south wall from 34.2 mm to 41.9 mm as can be noted by comparing the results obtained in Scenario 1 with Scenario 2 that depicted in Figures 10a and 10b. Figure 10c also shows that the piles under the Gate (Scenario 3) helped only a little as the maximum wall deflection would be reduced by only 1.2 mm, i.e., from 41.9 mm to 40.7 mm. The corresponding toe movements in the final stage in all the 3 scenarios vary from 5.1 mm to 5.8 mm and differ by less than 1 mm.

It can be noted by comparing Figure 10c with Figure 11b that the provision of the cross-walls reduces the maximum deflection of the south wall from 40.7 mm (Scenario 3) to 14.5 mm (Scenario 4). The maximum wall deflections have been reduced significantly by 2/3. The wall toe movements are also reduced from 5.8 mm to 4.2 mm. The cross-walls are thus proved to be indeed effective in reducing the wall deflections.

Proceedings DOI: 10.21467/proceedings.126
ISBN: 978-81-954993-7-3

Series: AIJR Proceedings
ISSN: 2582-3922

Table 4. Comparison of wall deflections in the final stage in different scenarios

Scenario		Section	Maximum wall deflection, mm				Notes
			South	Toe	North	Toe	
1	Free-field excavation	2	34.2	5.1	-34.2	-5.2	Positive and negative values denote movements toward north and south respectively.
2	With gate	2	41.9	5.7	-30.3	-4.5	
3	With gate/piles	2	40.7	5.8	-30.9	-4.4	
4	With gate/piles/cross-walls	2	14.5	4.2	-9.8	-2.8	
	(the benchmark case)	3	33.3	5.3	-30.9	-4.2	

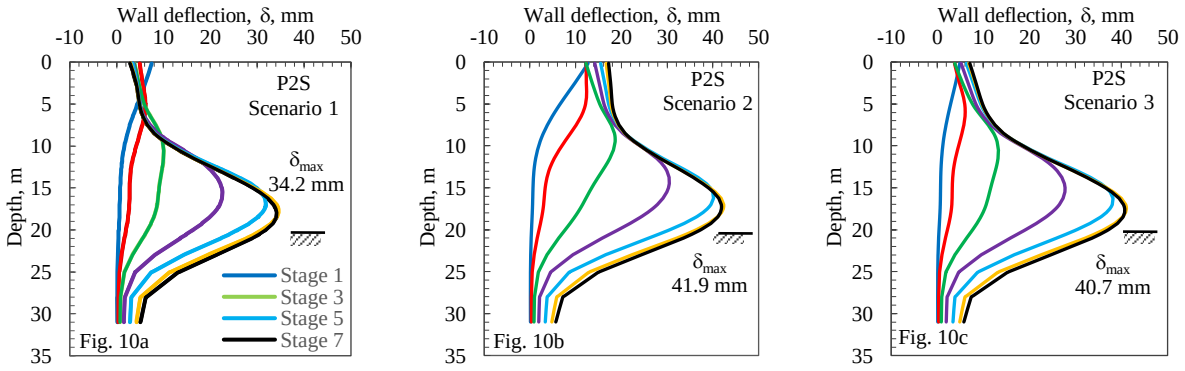

Figure 10: Wall Deflections at P2S obtained in the 3D analyses for Scenarios 1 to 3

5.2 Calibration the Results Against the Readings Obtained by Inclinometers SID-2 And SID-3

Scenario 4 is considered as the benchmark case for further comparisons. The wall deflection profiles obtained by Inclinometer SID-2, duly corrected for the toe movements, are shown in Figure 11a; and the profile at the end of excavation is compared with the profiles obtained from the numerical analyses in Figure 11b. The maximum wall deflection computed in the final stage is 14.5 mm, which is only 0.9 mm larger than 13.6 mm that observed in SID-2. As the calculated and the observed profiles are closely matched, it could be concluded that the soil parameters adopted, as depicted in Table 1, are appropriate.

Similarly, the wall deflection profiles obtained by SID-3, duly corrected for the toe movements, are shown in Figure 12a; and the measured profile at the end of excavation is compared with those obtained at Location P3N from the analyses in Figure 12b. The maximum deflection in the final stage is 30.9 mm, which is compatible with 30.4 mm that obtained by SID-3, with the readings duly corrected to account for the toe movements.

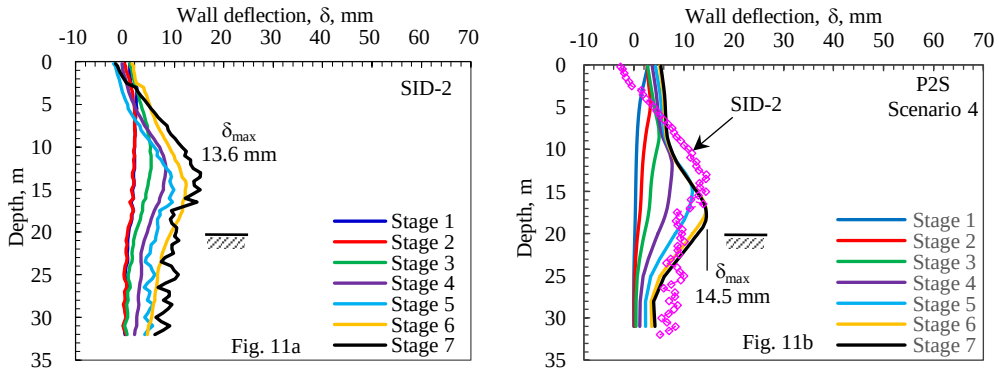

Figure 11: Observed and computed wall deflection profiles at Location P2S - Scenario 4

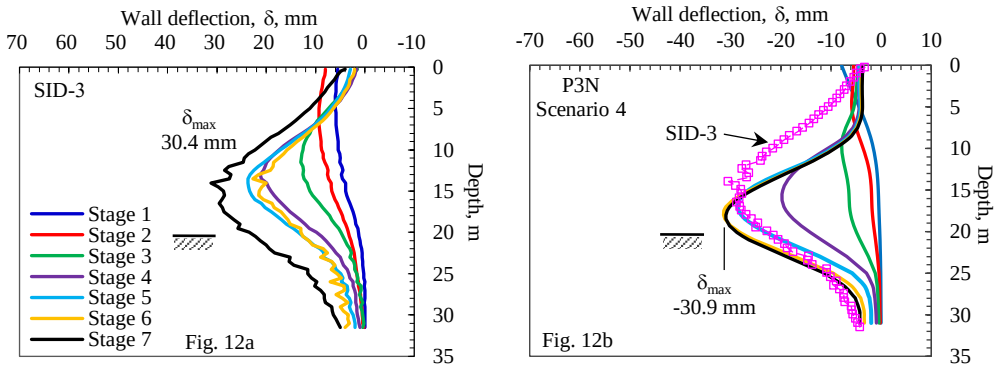

Figure 12: Observed and computed wall deflection profiles at Location P3N – Scenario 4

5.3 Effect of Imbalance of Earth-Pressures and Correction of Inclinometer Readings

The 3D numerical analyses show the occurrence of asymmetric wall deflections on the opposite sides of the excavation. Because of the imbalance of the earth-pressures on the two sides, the entire retaining system would have been pushed northward. As depicted in Figure 13, the longitudinal axis of the pit could move by as large as 22.4 mm at the first strut level in Section 2, where the gate is located, in Scenario 2 due to the surcharge load from the gate. Even with the support of the cross-wall in Scenario 4 (the full model), Figure 14 shows that the transverse movement of the axis of the retaining system would still be as large as 8.2 mm.

Even at a distance of about 12 m away from the edge of the Gate, Figure 15 still indicates a transverse movement of the axis of 3.0 mm in Section 3, refer to Figure 3 for location, in Scenario 4. These movements, caused by imbalance in earth-pressures, are quite significant in comparison with the maximum wall deflections computed in the analyses.

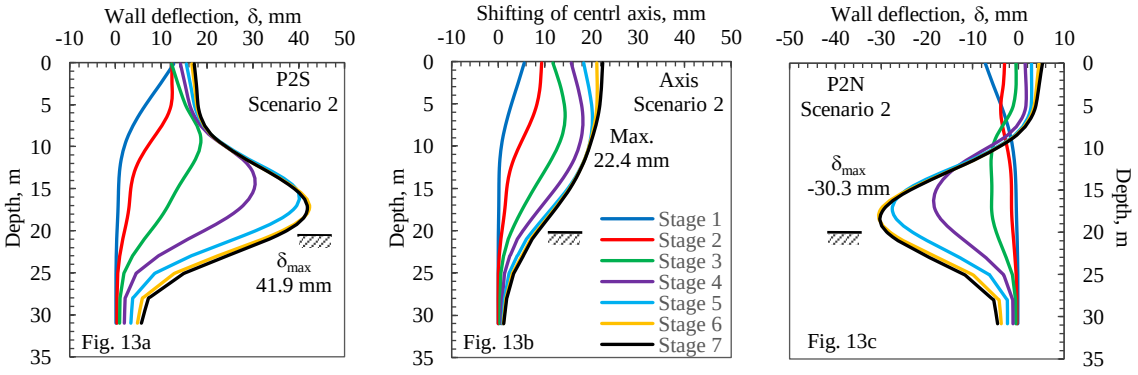

Figure 13: Effect of surcharge from the Gate to wall deflections at Section 2 without cross-wall - Scenario 2

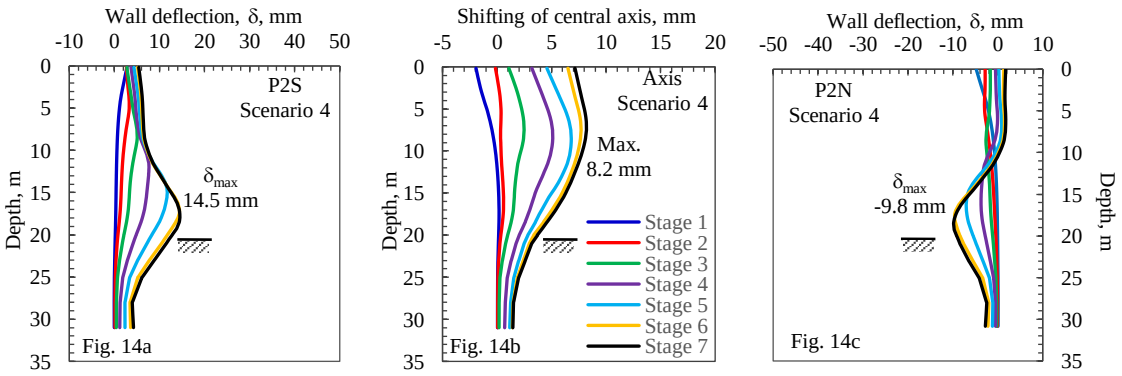

Figure 14: Effect of surcharge from the Gate to wall deflections at Section 2 with cross-wall - Scenario 4

Proceedings DOI: 10.21467/proceedings.126
ISBN: 978-81-954993-7-3

Series: AIJR Proceedings
ISSN: 2582-3922

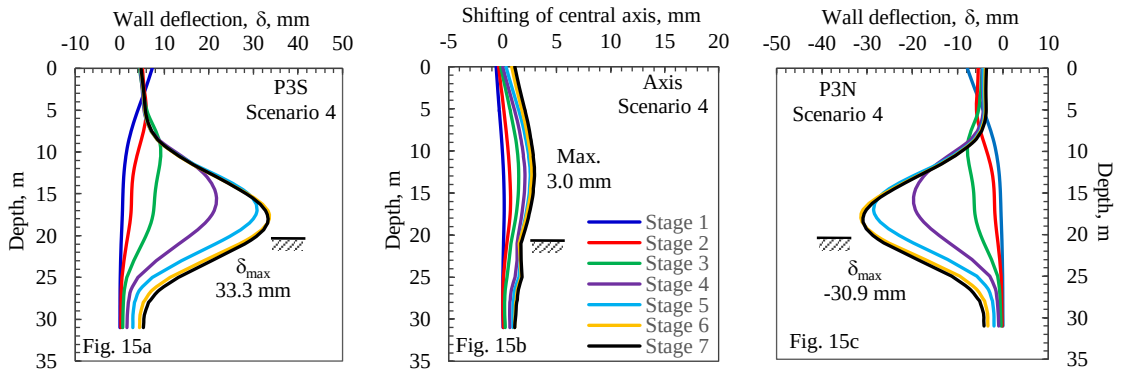

Figure 15: Effect of surcharge from the Gate to wall deflections at Section 3 with cross-wall - Scenario 4

It is thus inappropriate to correct inclinometer readings, as proposed by Hwang et al. (2007), by assuming the ends of the first-level struts to be unmoved once these struts are preloaded. Instead, the tips of the inclinometers (the diaphragm wall toes in this study) shall be assumed as the reference points for the purpose of making corrections. The readings of Inclinometers SID-2 and SID-3 presented in Figure 11a and Figure 12a have been corrected accordingly by adopting the computed toe deflections summarized in Table 4.

5.4 The Extent of the Influence of the Gate and the Cross-Walls

As shown in Figure 10 and Figure 11, the maximum wall deflections occur at around 18 m depth. Figure 16 shows the computed wall deflection profiles at the depth of 18 m along the south and the north wall in the final stage of excavation for Scenarios 2 and 4. Figure 16a shows that at Section 3, which is located at 21 m to the central axis of the Gate, the deflections at the south and the north wall are 36.3 mm and 32.2 mm respectively, with the difference of 4.1 mm. The difference in wall deflections diminishes at around 30 m from the edge of the Gate, where the computed largest deflections at the south and the north wall are 34.3 mm and 33.0 mm respectively, with the difference of 1.3 mm.

With the support of the cross-walls, Figure 16b shows that the deflections at Section 3 at the south and the north wall are 33.3 mm and 30.9 mm respectively, with the difference of 2.4 mm. The difference in wall deflections between the south and the north wall is still significant at Section 3, which is 14 m to the nearest cross-wall. At 39 m from the central axis of the Gate, the computed largest deflections at the south and at the north walls are 33.4 mm and 33.3 mm respectively. It is noted that the wall deflections at the mid-point between 2 cross-walls, at 3.5 m to the axis of the Gate, have similar values with those at Locations P2S and P2N.

Adopting the 1 mm difference as the criteria, the influence of the cross-wall would diminish at the distance of 26 m from the Gate, where the computed deflections at the south and the north wall are 33.7 mm and 32.7 mm respectively. The distance from the nearest cross-wall to the end of influence is 19 m, which is approximately 1.5 times of the width of excavation of 12 m. Understanding the influence of the cross-wall would enable rational design on the cross-walls such as determining the spacing, the thicknesses and the depths of the cross-wall panels.

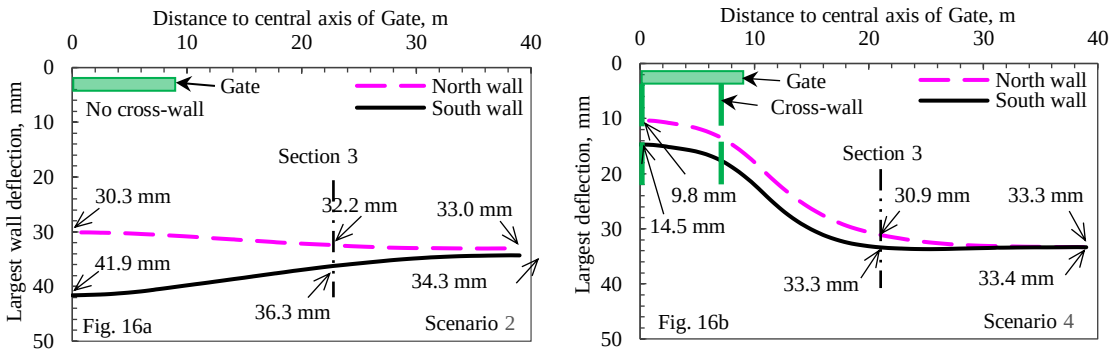

Figure 16: Largest wall deflection profiles along the south and the north wall in final stage - Scenarios 2 and 4

6 Conclusions

Based on results of two-dimensional and three-dimensional finite element analyses on an excavation braced with cross-walls using the non-linear Hardening-Soil constitutive model, the following conclusions could be drawn:

(1) Both the 2D and the 3D finite element models have been adopted in the analysis on the performance of the excavation for the cross-over tunnel. The matching between the computed wall deflection profiles with those observed in the inclinometers validates the soil parameters adopted for the Hardening-Soil model.

(2) Cross-walls are very effective in reducing wall deflections in deep excavations in soft deposits. The analyses show that the maximum wall deflections have been reduced approximately by 2/3, from 40.7 mm without cross-wall to 14.5 mm with cross-walls.

(3) The 3D analysis shows that the influence of the cross-walls extend to 19 m from the nearest cross-wall panel or approximately 1.5 times the width of excavation.

(4) Translation of the axis of the pit due to the imbalance of the earth-pressures on the two sides of the excavation shall be taken into account in making corrections to the inclinometer readings.

(5) The finite element analyses show that the toe movements of diaphragm walls are significant. In order to correctly interpret the inclinometer readings, the tips of the inclinometers shall be embedded in competent stratum such as the Jingmei Gravel or bedrock. Surveying the displacements at the tops of the inclinometers shall be carried out in case the toe anchorage in the competent stratum is not achieved.

(6) When the tops of inclinometer surveying results are not available, the inclinometer readings shall be corrected by taking the toes of the diaphragm walls at the reference points. The toe deflection values could be obtained from the numerical analysis.

(7) Struts preloading have significant influences on wall deflections and shall be adjusted in the analyses for the purpose of matching the inclinometer readings. In designs, it is proposed to adopt 50 % of the design preloads on struts so that the wall deflections computed could be close to the realistic conditions.

(8) Over-excavation by 1 m would increase the maximum wall deflections by 4 mm to 5 mm and a relaxation of preloads in struts by 50 % would have a similar effect of increase in wall deflections. Completely omission of the design preload would cause further 5 mm wall deflections. Workmanship is therefore an important factor influencing the performance of walls. Wall

Proceedings DOI: 10.21467/proceedings.126
ISBN: 978-81-954993-7-3

Series: AIJR Proceedings
ISSN: 2582-3922

deflections can be reduced by limiting the areas excavated, avoiding over-excavation and by preloading struts promptly.

The data presented above demonstrate how difficult it is to match the results of numerical analyses with the observations because wall deflections are affected by too many factors. Good agreement between the analyzed and the observed values cannot be ascertained either in designs and/or in back analyses. Good agreement can only be hoped but cannot be expected. On the other hand, as computer technology has been improved, user-friendly software packages are now available for, and the hardware is capable of, performing three-dimensional analyses of complicated soil-structural systems at affordable costs and efforts. This enables studies on the influences of numerous parameters on the performance of the retaining systems in deep excavations to be evaluated more accurately and with ease.

References

[1] Chin, C. T., Crooks, A. J. H. and Moh, Z. C. (1994). Geotechnical properties of the cohesive Sungshan deposits. *Geotechnical Engineering, J. Southeast Asian Geotechnical Society*, 25(2), 77-103. (in Chinese)

[2] Chin, C. T. and Liu, C-C. (1997). Volumetric and undrained behaviors of Taipei silty clay. *J. Chinese Institute of Civil and Hydraulic Engineering*, 9(4), 665-678. (in Chinese)

[3] Eide, O., Aas, G, and J□sang, T. (1972). Special application of cast-in-place slurry trench walls for tunnel in soft clay in Oslo. *Proc. 5 ECSMFE*, Vol. 1, Madrid 1972, 485-489.

[4] Hwang, R., Moh, Z. C. and Hu, I-C. (2013). Effects of Consolidation and specimen disturbance on strengths of Taipei Clays, *Geotechnical Engineering, J. of SEAGS & AGSSEA*, v44, no. 1, March, Bangkok, 9-18.

[5] Hwang, R. N. and Wong, L. W. (2018a). Effects of preloading of struts on retaining structures in deep excavations. *Geotechnical Engineering, J. of SEAGS & AGSSEA*, June, 49(2), 104-114.

[6] Hwang, R. N., Wang, C-H, and Wong, L. W. (2018b). Verification of back analyses of deep excavations and applications of wall deflection paths. *Sino-Geotech, J. Sino-Geotechnics Research and Development Foundation*, March, 155, 101-116. (in Chinese)

[7] Karlsrud, K. and Andresen, L. (2008). Design and performance of deep excavations in soft clays. *6th International Conference on Case Histories in Geotechnical Engineerin*g, Arlington, VA. August 11-16.

[8] Lee, S. H. (1996). Engineering geological zonation for the Taipei City. *Sino-Geotechnics, J. Sino-Geotechnics Research and Development Foundation*, March, 54, 25-34. (in Chinese)

[9] Li, C. L. (2011). *The beauty of Taipei architecture*. https://mypaper.pchome.com.tw/tfjxb/post/1322383095/? Show_map=1 (in Chinese).

[10] MAA (1987). *Engineering characteristics of Taipei Clay*. Taipei, Taiwan: MAA Group Consulting Engineers, Taipei.

[11] Moh, Z. C. and Ou C. D. (1979). Engineering characteristics of Taipei Silt. *Proc., 6th Asian Regional Conference on Soil Mechanics and Foundation Engineering*, Singapore, 1, 155-158.

[12] Ou, C.Y., Lin, Y.L. and Hsieh, P.G. (2006). Case record of an excavation with cross-walls and buttress walls. *Journal of GeoEngineering*, Vol. 1, No. 2, December.79-86.

[13] PLAXIS, B. V. (2013). *PLAXIS reference manual*. Plaxis BV, Delft, the Netherlands.

[14] Schanz, T. and Vermeer, P. A. (1998). On the Stiffness of Sands. *Pre-failure Deformation Behaviour of Geomaterials*, ICE, London, UK, 1998.

[15] Schanz, T., Vermeer, P.A. and Bonnier, P.G. (1999). The hardening soil model: formulation and verification. *Beyond 2000 in Computational Geotechnics*. Rotterdam. 281-290.